


Article

Hyperbranched Polycarbosiloxanes: Synthesis by Piers-Rubinsztajn Reaction and Application as Precursors to Magnetoceramics

Huayu Zhang ^{1,2}, Lei Xue ³, Jianquan Li ^{1,2} and Qingyu Ma ^{1,2,*} 

¹ Shandong Provincial Key Laboratory of Preparation and Measurement of Building Materials, University of Jinan, Jinan 250022, China; zhy2327212@163.com (H.Z.); mse_ljq@ujn.edu.cn (J.L.)

² School of Materials Science and Engineering, University of Jinan, Jinan 250022, China

³ Beijing Institute of Aeronautical Materials, Beijing 100095, China; xuelei282@163.com

* Correspondence: mse_maqy@ujn.edu.cn

Received: 22 February 2020; Accepted: 16 March 2020; Published: 17 March 2020



Abstract: Silicon-containing hyperbranched polymers (Si-HBPs) have drawn much attention due to their promising applications. However, the construction of Si-HBPs, especially those containing functional aromatic units in the branched backbones by the simple and efficient Piers-Rubinsztajn (P-R) reaction, has been rarely developed. Herein, a series of novel hyperbranched polycarbosiloxanes were prepared by the P-R reactions of methyl-, or phenyl-triethoxysilane and three Si-H containing aromatic monomers, including 1,4-bis(dimethylsilyl)benzene, 4,4'-bis(dimethylsilyl)-1,1'-biphenyl and 1,1'-bis(dimethylsilyl)ferrocene, using $B(C_6F_5)_3$ as the catalyst for 0.5 h at room temperature. Their structures were fully characterized by Fourier transform infrared spectroscopy, 1H NMR, ^{13}C NMR, and ^{29}Si NMR. The molecular weights were determined by gel permeation chromatography. The degrees of branching of these polymers were 0.69–0.89, which were calculated based on the quantitative ^{29}Si NMR spectroscopy. For applications, the ferrocene-linked Si-HBP can be used as precursors to produce functional ceramics with good magnetizability after pyrolysis at elevated temperature.

Keywords: hyperbranched polymers; Piers–Rubinsztajn reaction; polycarbosiloxanes; magnetic ceramics

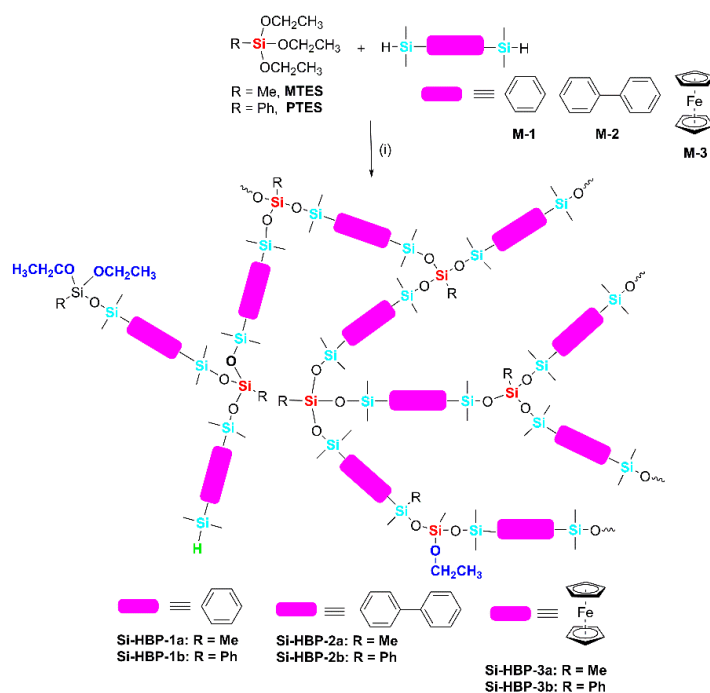
1. Introduction

Hyperbranched polymers (HBPs), which are defined as highly branched three-dimensional macromolecules, have attracted great attention, due to their unique structures and properties such as abundant functional groups, intramolecular cavities, low viscosity and high solubility, and extensive applications in photoelectric materials, coatings, adhesives, membranes, sensors, catalysis and biomaterials [1–7]. Among these HBPs, silicon-containing HBPs (Si-HBPs) are one of most important species and have attracted specific interest due to their potentials as silicon carbide ceramic precursors, degradable template molecules, optical materials, modifiers of composites, cell imaging, drug delivery, and gas chromatography [8–15]. The Si-HBPs can be prepared by several strategies, including hydrosilylation reactions from silicon-containing monomers containing Si–H bonds and unsaturated bonds (e.g., vinyl or alkynyl) [16,17], organometallic reaction (e.g., Grignard reaction) [13,18] and polycondensation reaction [19]. However, these strategies have some disadvantages. For example, the most commonly used hydrosilylation reaction requires noble metal-based catalysts, typically Platinum-based Speier’s and Karstedt’s catalysts, and can be affected by moisture and not tolerant for some functional groups. The organometallic reactions are sensitive to moisture and air. To overcome these drawbacks, we and other researchers have introduced click reactions to prepare Si-HBPs [12,20,21].

For example, Wu et al. developed a one-pot thiol-ene approach to prepare polyhedral oligomeric silsesquioxane (POSS)-embedded HBPs with tunable POSS units and terminal vinyl groups from an AB₇ POSS monomer [12]. We used the step-growth thiol-ene reaction to prepare Si-HBPs from mercaptopropylmethylallylsilane (AB₂) or mercaptopropyltriallylsilane (AB₃) as the hyperbranched monomers [21]. However, compared to diversified synthetic strategies for conventional HBPs, the strategies for the synthesis of Si-HBPs are still limited. In particular, developing Si-HBPs via simple, rapid and mild synthetic procedures is highly desirable.

The Piers–Rubinsztajn (P–R) reaction, namely the condensation of alkoxy silanes with hydrosilanes, has rapidly developed since it was found in the 1990s [22,23], because this strategy is mild and provides a possibility for the controlled or precise synthesis of silicones, including small molecules, linear polymers, and crosslinked materials [24–31]. For example, the P–R coupling reactions of various organic tris(dimethylsiloxy)silane and trialkoxysilane compounds can generate a series of cyclic polysiloxanes with cyclotetrasiloxane subunits in a simple one-step synthesis [32]. Matsumoto et al. presented a highly selective sequence-controlled synthesis of linear, branched, and cyclic oligosiloxanes by the iteration of tris(pentafluorophenyl)borane (B(C₆F₅)₃)-catalyzed P–R reaction and hydrosilylation of carbonyl compounds [33]. The P–R reaction has also been applied to synthesize Si-HBPs [34–37]. For example, Liu et al. reported hyperbranched POSS-based polymers with ultra-high molecular weight by the P–R reaction between octakis(dimethylsiloxy)octa-silsesquioxane with different dialkoxy silanes [34]. However, compared to other synthetic strategies for Si-HBPs, the reports on Si-HBPs, in particular those containing functional aromatic units in the branched backbones prepared by the P–R reaction are still few.

Herein, we present a series of novel hyperbranched polycarbosiloxanes, Si-HBP-1 to Si-HBP-3, based on methyl-, or phenyl-triethoxysilane and three Si–H containing aromatic monomers, including 1,4-bis(dimethylsilyl)benzene (M-1), 4,4′-bis(dimethylsilyl)-1,1′-biphenyl (M-2) and 1,1′-bis(dimethylsilyl) ferrocene (M-3), in the presence of B(C₆F₅)₃ as the catalyst by the P–R reactions (Scheme 1). The obtained Si-HBPs were fully characterized by Fourier transform infrared spectroscopy (FT-IR), ¹H NMR, ¹³C NMR, ²⁹Si NMR and gel permeation chromatography (GPC). Moreover, the pyrolysis of ferrocene-based polycarbosiloxanes at elevated temperatures can afford novel nanostructured ceramics with good magnetizability in a high yield.



Scheme 1. Synthetic routes of hyperbranched polycarbosiloxanes, Si-HBP-1 to Si-HBP-3, by the Piers–Rubinsztajn reaction. (i): B(C₆F₅)₃, toluene, room temperature, 30 min.

2. Materials and Methods

2.1. Materials and Characterization

Unless otherwise noted, all reagents were obtained from commercial suppliers and used without further purification. Toluene was dried by distillation from the sodium ketyl of benzophenone. Fourier transform infrared (FT-IR) spectra of the products were recorded on a Bruker Tensor27 spectrophotometer (Ettlingen, Germany) in the frequency range 4000–400 cm^{-1} at a resolution of 4 cm^{-1} with a total of 32 scans. ^1H NMR and ^{13}C NMR spectra were measured on a Bruker AVANCE-300 or 400 NMR spectrometer (Karlsruhe, Germany), with CDCl_3 as the solvent. Quantitative ^{29}Si NMR spectroscopy (Karlsruhe, Germany) was performed using an inverse gated ^1H -decoupling sequence. Samples were prepared in $\text{Cr}(\text{acac})_3/\text{CDCl}_3$ solution (0.1 M $\text{Cr}(\text{acac})_3$). The molecular weights of the polymers and their polydispersity indices (PDI, M_w/M_n) were determined by a Waters 1515 gel permeation chromatography (GPC) system equipped with a refractive index detector (Milford, MA, USA), using monodisperse polystyrene (PS) as calibration standards and THF containing 0.05 M LiBr as the eluent at a flow rate of 1.0 mL min^{-1} . Thermogravimetric analysis (TGA) was performed using a TA SDTQ600 (Columbus, OH, USA) with a heating rate of 10 $^\circ\text{C}/\text{min}$ from room temperature to 1000 $^\circ\text{C}$ under N_2 . Differential scanning calorimetry (DSC) was performed on a Netzsch DSC 204 Phoenix (Columbus, OH, USA) and measurements were done under nitrogen atmosphere at a heating rate of 10 $^\circ\text{C}/\text{min}$ from -160°C to room temperature. X-ray diffraction (XRD) experiments were performed on a Philips PW 2830 X-ray powder diffractometer (Karlsruhe, Germany), with monochromatized $\text{Cu K}\alpha$ radiation ($\lambda = 1.5406 \text{ \AA}$). Magnetization curves were performed by using a Lake Shore 7037/9509-P vibrating sample magnetometer at room temperature.

2.2. Synthesis of Si-H Containing Aromatic Monomers

1,4-Bis(dimethylsilyl)benzene (M-1), 4,4'-bis(dimethylsilyl)-1,1'-biphenyl (M-2) and 1,1'-bis(dimethylsilyl)ferrocene (M-3) were prepared according to previous reports [17,38].

For M-1: IR (KBr pellet cm^{-1}): 3047, 2959, 2907, 2123, 1417, 1381, 1250, 1130, 870, 828, 755, 724, 656, 625, 484, 469. ^1H NMR (400 MHz, CDCl_3) δ 7.64 (s, 4H), 4.55–4.51 (m, 2H), 0.44 (s, 12H). ^{13}C NMR (100 MHz, CDCl_3): δ 137.6, 132.5, -4.7 . ^{29}Si NMR (75 MHz, CDCl_3): δ -17.05 .

For M-2: IR (KBr pellet cm^{-1}): 3047, 2955, 2123, 1598, 1397, 1253, 1116, 876, 745, 728, 525. ^1H NMR (400 MHz, CDCl_3) δ 7.69 (dd, 8H), 4.58–4.55 (m, 2H), 0.45 (d, 12H). ^{13}C NMR (100 MHz, CDCl_3): δ 141.8, 136.4, 134.5, 128.7, 127.0, 126.6, -3.7 . ^{29}Si NMR (75 MHz, CDCl_3): δ -17.12 .

For M-3: ^1H NMR (400 MHz, CDCl_3) δ 7.69 (dd, 8H), 4.58–4.55 (m, 2H), 0.45 (d, 12H). ^{13}C NMR (100 MHz, CDCl_3): δ 73.8, 71.7, 68.3, -3.0 . ^{29}Si NMR (75 MHz, CDCl_3): δ -16.85 .

2.3. Synthesis of Si-H Containing Aromatic Monomers

All the hyperbranched polycarbosiloxanes were prepared from methyl-, or phenyl-triethoxysilane and Si-H containing aromatic monomers with approximately equimolar amounts of ethoxy groups and Si-H groups. Attention: there was a relatively large amount of bubbles and exotherm during the process.

Si-HBP-1a: A 250 mL flask was charged with 100 mL toluene, M-1 (1.50 g, 7.48 mmol) and $\text{B}(\text{C}_6\text{F}_5)_3$ (0.5 mol % of Si-H group, 0.0197g, 0.0375 mmol). The mixture was stirred at room temperature for 5 min. Methyltriethoxysilane (MTES, 0.9077g, 4.99 mmol) in toluene (10 mL) was slowly added into the mixture. After a short induction period, gas was vigorously evolved from the solution with heat release. The reaction mixture was stirred at room temperature for 30 min and neutral alumina (~ 1 g) was added into the mixture. The resulting slurry was stirred for another 20 min, after which alumina was removed by vacuum filtration. The filtrate was distilled under vacuum to remove residual solvent and starting materials, affording the final product as a colorless and viscous liquid (1.90 g, yield: 86%). IR (KBr pellet cm^{-1}): 3052, 2959, 1248, 1139, 1041, 819, 772, 669, 612. ^1H NMR (400 MHz, CDCl_3) δ 7.72–7.59 (m, $-\text{SiC}_6\text{H}_4-$), 7.48–7.42 (m, $-\text{SiC}_6\text{H}_4-$), 3.85 (d, $-\text{SiOCH}_2\text{CH}_3$), 1.34–1.27 (m, $-\text{SiOCH}_2\text{CH}_3$),

0.48–0.02 (m, $-\text{SiCH}_3$). ^{13}C NMR (100 MHz, CDCl_3): δ 140.6, 140.3, 139.9, 132.5, 132.4, 57.9, 18.3, 0.98, 0.73, 0.64, 0.50, -1.85, -3.52. ^{29}Si NMR (75 MHz, CDCl_3): δ -0.91, -1.23, -1.67, -1.74, -1.95, -2.11, -2.26, -56.67, -57.16, -63.89, -64.34, -64.63. Anal. Calcd for $\text{C}_{16}\text{H}_{27}\text{O}_3\text{Si}_4$: C, 50.61; H, 7.17. Found: C, 50.81; H, 7.95.

Si-HBP-1b: The synthesis and post-treatment procedures of Si-HBP-1b were similar to those of Si-HBP-1a, except that MTES was replaced by phenyltriethoxysilane (PTES, 1.2230 g, 4.99 mmol). The product was afforded as a colorless and viscous liquid (2.1 g, yield: 84%). IR (KBr pellet cm^{-1}): 3057, 3006, 2959, 1428, 1377, 1258, 1134, 1041, 814, 772, 720, 694, 674, 612, 555. ^1H NMR (400 MHz, CDCl_3) δ 7.69–7.60 (m, $-\text{SiC}_6\text{H}_4-$, $-\text{SiC}_6\text{H}_5$), 7.53–7.28 (m, $-\text{SiC}_6\text{H}_4-$, $-\text{SiC}_6\text{H}_5$), 3.84 (d, $-\text{SiOCH}_2\text{CH}_3$), 1.28–1.20 (m, $-\text{SiOCH}_2\text{CH}_3$), 0.47–0.07 (m, $-\text{SiCH}_3$). ^{13}C NMR (100 MHz, CDCl_3): δ 140.1, 139.9, 134.3, 134.2, 134.0, 132.6, 132.4, 130.1, 129.9, 129.8, 129.7, 129.1, 128.3, 127.9, 127.7, 127.6, 58.6, 58.5, 18.2, 0.96, 0.83, 0.71, 0.67, 0.50, 0.48, 0.42. ^{29}Si NMR (75 MHz, CDCl_3): δ -0.46, -0.51, -0.67, -0.94, -1.26, -70.71, -71.15, -78.04, -78.08. Anal. Calcd for $\text{C}_{21}\text{H}_{29}\text{O}_3\text{Si}_4$: C, 57.09; H, 6.62. Found: C, 57.24; H, 7.70.

Si-HBP-2a: 4,4'-Bis(dimethylsilyl)-1,1'-biphenyl (M-2, 1.50 g, 5.54 mmol), $\text{B}(\text{C}_6\text{F}_5)_3$ (0.0146 g, 0.0277 mmol) and MTES (0.6726 g, 3.70 mmol) were used to prepare Si-HBP-2a. The synthesis and post-treatment procedures were similar to those of Si-HBP-1a. The product was afforded as a colorless and viscous liquid (1.8 g, yield: 89%). IR (KBr pellet cm^{-1}): 3067, 3016, 2959, 2923, 1744, 1594, 1532, 1480, 1434, 1382, 1248, 1123, 1036, 1000, 813, 778, 721, 695, 632, 560. ^1H NMR (400 MHz, CDCl_3) δ 7.83–7.73 (m, $-\text{SiC}_6\text{H}_4-\text{C}_6\text{H}_4\text{Si}-$), 7.64–7.60 (m, $-\text{SiC}_6\text{H}_4-\text{C}_6\text{H}_4\text{Si}-$), 7.57–7.53 (m, $-\text{SiC}_6\text{H}_4-\text{C}_6\text{H}_4\text{Si}-$), 3.97–3.89 (m, $-\text{SiOCH}_2\text{CH}_3$), 1.43–1.32 (m, $-\text{SiOCH}_2\text{CH}_3$), 0.58–0.16 (m, $-\text{SiCH}_3$). ^{13}C NMR (100 MHz, CDCl_3): δ 142.1, 141.5, 140.9, 138.5, 138.4, 138.2, 138.1, 138.0, 134.1, 133.9, 133.8, 133.7, 129.1, 128.4, 126.6, 126.5, 126.4, 126.3, 126.1, 58.2, 58.1, 18.5, 18.4, 1.1, 0.9, 0.8, 0.7, -1.8, -3.4, -5.1. ^{29}Si NMR (75 MHz, CDCl_3): δ -0.87, -1.39, -1.42, -1.63, -1.75, -1.93, -48.35, -56.58, -56.89, -63.76, -64.06, -64.11. Anal. Calcd for $\text{C}_{25}\text{H}_{33}\text{O}_3\text{Si}_4$: C, 60.80; H, 6.74. Found: C, 60.99; H, 8.12.

Si-HBP-2b: The synthesis and post-treatment procedures of Si-HBP-2b were similar to those of Si-HBP-2a, except that MTES was replaced by PTES (0.9068 g, 3.70 mmol). The product was afforded as a colorless and viscous liquid (1.91 g, yield: 84%). IR (KBr pellet cm^{-1}): 3067, 3021, 2954, 2928, 1744, 1599, 1486, 1428, 1248, 1124, 1036, 996, 824, 777, 721, 700, 632, 555. ^1H NMR (400 MHz, CDCl_3) δ 7.75–7.39 (m, $-\text{SiC}_6\text{H}_4-\text{C}_6\text{H}_4\text{Si}-$, $-\text{SiC}_6\text{H}_5$), 3.97–3.89 (m, $-\text{SiOCH}_2\text{CH}_3$), 1.35–1.26 (m, $-\text{SiOCH}_2\text{CH}_3$), 0.55–0.09 (m, $-\text{SiCH}_3$). ^{13}C NMR (100 MHz, CDCl_3): δ 142.0, 141.5, 141.0, 138.1, 138.0, 134.6, 134.3, 134.0, 133.8, 133.7, 133.6, 130.1, 130.0, 128.0, 127.9, 127.8, 126.6, 126.5, 126.3, 126.1, 58.7, 58.6, 18.4, 18.3, 1.1, 0.80, 0.65. ^{29}Si NMR (75 MHz, CDCl_3): δ 0.21, -0.22, -0.27, -0.44, -0.64, -0.95, -63.93, -70.95, -77.72, -77.85. Anal. Calcd for $\text{C}_{30}\text{H}_{35}\text{O}_3\text{Si}_4$: C, 64.81; H, 6.35. Found: C, 64.34; H, 7.15.

Si-HBP-3a: 1,1'-Bis(dimethylsilyl)ferrocene (M-3, 2.00 g, 6.62 mmol), $\text{B}(\text{C}_6\text{F}_5)_3$ (0.0174 g, 0.0331 mmol) and MTES (0.8023 g, 4.41 mmol) were used to prepare Si-HBP-3a. The synthesis and post-treatment procedures were similar to those of Si-HBP-1a. The product was afforded as a colorless and viscous liquid (1.90 g, yield: 72%). IR (KBr pellet cm^{-1}): 3088, 2959, 2897, 1418, 1356, 1248, 1165, 1036, 959, 901, 813, 773, 689, 669, 622. ^1H NMR (400 MHz, CDCl_3) δ 4.39–4.15 (m, $-\text{C}_5\text{H}_4\text{FeC}_5\text{H}_4-$), 3.89–3.74 (m, $-\text{SiOCH}_2\text{CH}_3$), 1.29–1.19 (m, $-\text{SiOCH}_2\text{CH}_3$), 0.44–0.29 (m, $-\text{SiCH}_3$). ^{13}C NMR (100 MHz, CDCl_3): δ 73.7, 73.6, 73.4, 73.2, 73.1, 73.0, 72.9, 71.7, 71.2, 70.9, 70.8, 70.7, 68.4, 68.0, 58.0, 18.4, 18.3, 1.9, 1.7, 1.4, 1.3, 1.2, 0.2, -2.0, -3.4. ^{29}Si NMR (75 MHz, CDCl_3): δ 1.53, 1.26, 0.87, 0.78, 0.58, 0.38, 0.29, 0.23, 0.16, -0.03, -0.53, -49.84, -57.42, -57.48, -58.70, -64.99, -66.22, -66.27. Anal. Calcd for $\text{C}_{22}\text{H}_{33}\text{O}_3\text{Si}_4\text{Fe}_{1.5}$: C, 48.79; H, 6.14. Found: C, 49.81; H, 7.51.

Si-HBP-3b: The synthesis and post-treatment procedures of Si-HBP-3b were similar to those of Si-HBP-3a, except that MTES was replaced by PTES (1.0602 g, 4.41 mmol). The product was afforded as a colorless and viscous liquid (2.14 g, yield: 74%). IR (KBr pellet cm^{-1}): 3093, 3073, 2959, 2897, 1651, 1591, 1428, 1367, 1300, 1253, 1168, 1129, 1036, 959, 897, 808, 778, 736, 721, 700, 674, 632, 566. ^1H NMR (400 MHz, CDCl_3) δ 7.76–7.29 (m, $-\text{SiC}_6\text{H}_5$), 4.40–4.05 (m, $-\text{C}_5\text{H}_4\text{FeC}_5\text{H}_4-$), 3.82–3.73 (m, $-\text{SiOCH}_2\text{CH}_3$), 1.27–1.21 (m, $-\text{SiOCH}_2\text{CH}_3$), 0.49–0.01 (m, $-\text{SiCH}_3$). ^{13}C NMR (100 MHz, CDCl_3): δ 134.6, 134.4, 134.1, 130.1, 129.8, 129.5, 127.8, 127.7, 127.6, 127.4, 73.6, 73.5, 73.4, 73.3, 73.2, 72.1, 71.3, 71.2,

70.9, 70.8, 68.4, 58.6, 58.5, 58.4, 18.4, 2.1, 1.8, 1.7, 1.4, 1.2, 0.2. ^{29}Si NMR (75 MHz, CDCl_3): δ 2.67, 2.48, 2.45, 2.08, 1.94, 1.81, 1.78, 1.48, 1.29, 1.13, 0.95, 0.82, 0.03, -64.40, -71.49, -72.02, -78.68, -79.84. Anal. Calcd for $\text{C}_{27}\text{H}_{35}\text{O}_3\text{Si}_4\text{Fe}_{1.5}$: C, 53.72; H, 5.84. Found: C, 54.63; H, 7.52.

2.4. Synthesis of Magnetic Ceramics from Si-HBP-3a

Si-HBP-3a was pyrolyzed at 900 °C for 2 h in a tube furnace with the heating rate of 10 °C/min from temperature to 600 °C, and 5 °C/min from 600 to 900 °C under the flowing nitrogen and then cooled to temperature. The product was obtained as a black powder.

3. Results and Discussion

3.1. Synthesis

The Si-H containing monomers, M-1 to M-3, were synthesized following the literature procedures [17,38]. Their structures were characterized by ^1H NMR, ^{13}C NMR, and ^{29}Si NMR and the satisfactory analysis data were obtained.

The synthetic routes of silicon-containing HBPs, Si-HBP-1 to Si-HBP-3, were shown in Scheme 1. All the polymers were synthesized by the P-R polymerization reactions of trifunctional ethoxy monomer (MTES and PTES) and bifunctional Si-H monomers (M-1 to M-3). The molar feed ratio of ethoxy groups and Si-H groups was set at approximately 1:1. It is known that controlling the gel time is crucial for the preparation of hyperbranched polymers. Taking the P-R reaction of M-1 and MTES as an example (Si-HBP-1a), different amounts of catalysts, including 0.2, 0.5, 0.8 and 1.0 mol % (calculation based on the amount of Si-H groups), were used to evaluate the reaction rate, while keeping the concentration of reaction mixture constant. Table 1 shows the gel time variation by changing the amount of catalyst. It was found that when the amount is 0.2 mol %, the reaction was very slow and the gel time is ca. 5 h. When the amounts are 0.8 and 1.1 mol %, the reactions were difficult to control and the solutions rapidly became gel. Thus, 0.5 mol % was chosen as the catalyst amount for the reaction. In addition, it was found that after 30 min, the gelation also occurred and the reaction time was selected to be 30 min. All the products were afforded as colorless and viscous liquids and soluble in aliphatic and aromatic solvents.

Table 1. The gel time versus catalyst amount for the preparation of Si-HBP-1a.

Entry	The Mount of Catalyst (mol %)	Gel Time
1	0.2	ca. 5 h
2	0.5	32 min
3	0.8	< 30 s
4	1.1	< 20 s

3.2. Characterization

The structures of all the polymers were fully determined by FT-IR, ^1H NMR, ^{13}C NMR, ^{29}Si NMR, and elemental analysis. The FT-IR spectra of these polymers were shown in Figure 1 and Figure S1 (Supplementary Materials). The absorption peaks, with moderate intensity ranging from 1650 to 1400 cm^{-1} , are associated with C=C stretching vibrations from phenyl or cyclopentadienyl (Cp) units in the networks. The peaks at ca. 1265 cm^{-1} are attributed to the deformation vibrations of methyl groups linked to silicon atoms. Compared with the monomers (taking M-1 as an example), the strong absorption band at 2123 cm^{-1} attributed to the Si-H stretching vibration disappears in the spectrum of Si-HBP-1a, while a new and strong peak at ca. 1035 cm^{-1} undoubtedly assigned to the characteristic Si-O-Si stretching vibration is observed (Figure S2 in Supplementary Materials). Similar results are also obtained in other polymers. This finding reveals that most of the Si-H groups have been consumed after the polymerization reaction, thereby indicating that the target polymers have been successfully synthesized.

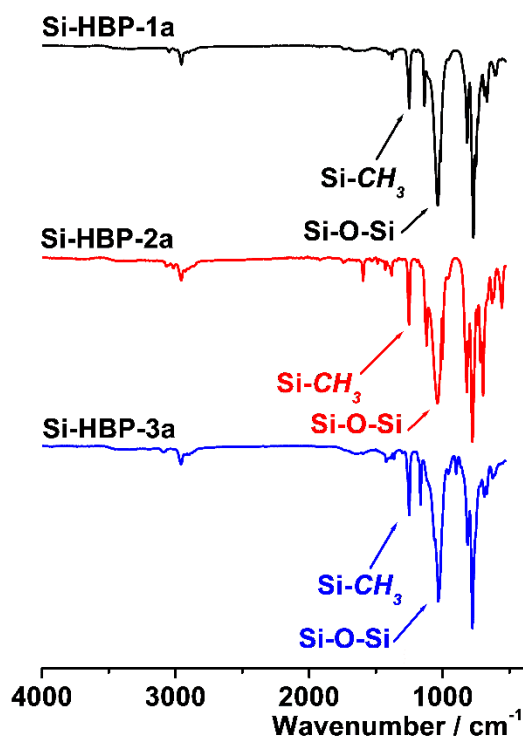


Figure 1. Fourier transform infrared (FT-IR) spectroscopy of Si-HBP-1a, Si-HBP-2a and Si-HBP-3a.

Figure 2 and Figure S3 (Supplementary Materials) show the ^1H NMR spectra of these polymers in CDCl_3 and the assignments of the resonance signals. Similar to other hyperbranched polymers, these polymers also possess dendritic (D), linear (L) and terminal (T) units [5]. Compared to the starting monomers (M-1 to M-3), the characteristic signals of proton on Si–H bond (4.51–4.58 ppm, see the experimental section) in these polymers approximately disappeared. Meanwhile, the signals, which are assigned to the protons in the ethoxy groups, also nearly disappeared and weak peaks at ca. 3.9–3.8 ppm (H_f and H_{f1} in Figure 2a, H_g and H_{g1} in Figure 2b, H_f and H_{f1} in Figure 2c) and 1.4–1.3 ppm (H_g and H_{g1} in Figure 2a, H_h and H_{h1} in Figure 2b, H_g and H_{g1} in Figure 2c) were observed for the protons associated with the secondary carbon $-\text{SiOCH}_2\text{CH}_3$ and the primary carbon $-\text{SiOCH}_2\text{CH}_3$. The almost disappearance of Si–H bonds and $-\text{OCH}_2\text{CH}_3$ groups suggested the successful reactions from the starting materials and both of them have occupied the terminal positions in the networks. For the polymers based on methyltriethoxysilane and M-1 to M-3, the peaks at 0–0.5 ppm are obviously attributed to the protons of Si– CH_3 groups. The signals from 7.2 ppm to 7.8 ppm are assigned to the aromatic protons from the phenyl groups for all the polymers except Si-HBP-3a. For Si-HBP-3a and Si-HBP-3b, the signals at around 4.15 ppm and 4.35 ppm corresponded to the protons on the Cp rings (Figure 2c and Figure S3c in Supplementary Materials). Moreover, for Si-HBP-3b, the multiple peaks in the region of 7.2–7.8 ppm arising from the phenyl units (Figure 3c) proved that it was synthesized from PTES, which is different from that of Si-HBP-3a.

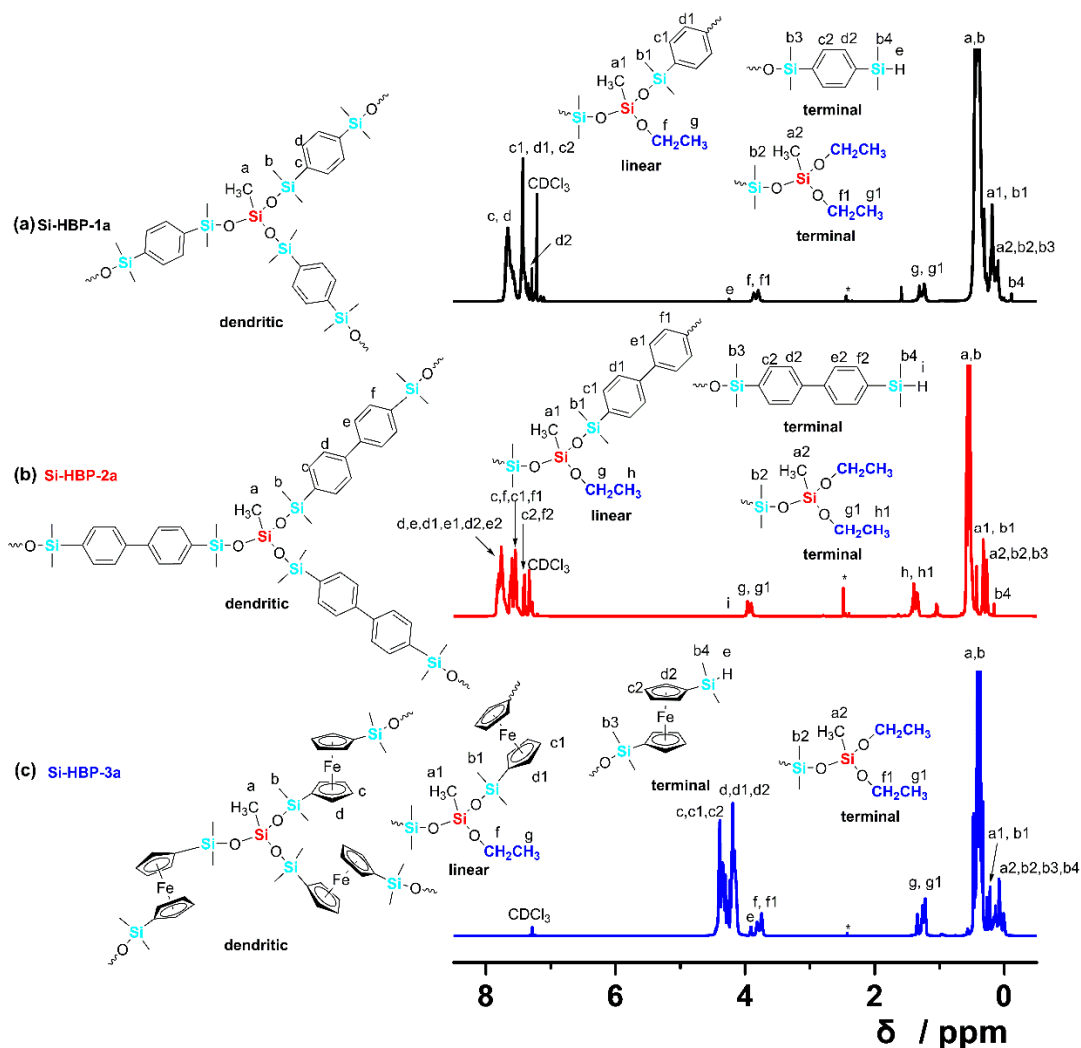


Figure 2. ^1H NMR spectra of Si-HBP-1a (a), Si-HBP-2a (b) and Si-HBP-3a (c). The asterisk denotes the residual toluene in the product.

Further evidence can be found in ^{13}C NMR spectra of these polymers in CDCl_3 with the assignments of the resonance signals (Figure 3 and Figure S4 in Supplementary Materials). Similar to the results in ^1H NMR spectra, the characteristic signals of $-\text{SiOCH}_2\text{CH}_3$ carbons are found at ca. 58 ppm (C_g and C_{g1} in Figure 3a, C_j and C_{j1} in Figure 3b, C_f and C_{f1} in Figure 3c) and 18 ppm (C_h and C_{h1} in Figure 3a, C_k and C_{k1} in Figure 3b, C_g and C_{g1} in Figure 3c) from the secondary carbon $-\text{SiOCH}_2\text{CH}_3$ and the primary carbon $-\text{SiOCH}_2\text{CH}_3$. As expected, the multiple peaks from -5 ppm to 3 ppm are associated with the carbons from the $-\text{Si}-\text{CH}_3$ units depending on the chemical environments. The signals in the region of 142 – 126 ppm are assigned to sp^2 phenyl carbon atoms from the M-1 to M-3, or PTES for all the polymers except Si-HBP-3a. For the ferrocene-linked polymers (Si-HBP-3a and Si-HBP-3b), the characteristic signals for the carbons on the C_p rings are observed at ca. 68 ppm and 73 ppm (Figure 3c and Figure S4c in Supplementary Materials). For Si-HBP-3b, the introduction of phenyl groups in the network can also be proven by the multiple peaks in the region of 135 – 127 ppm (Figure S4c).

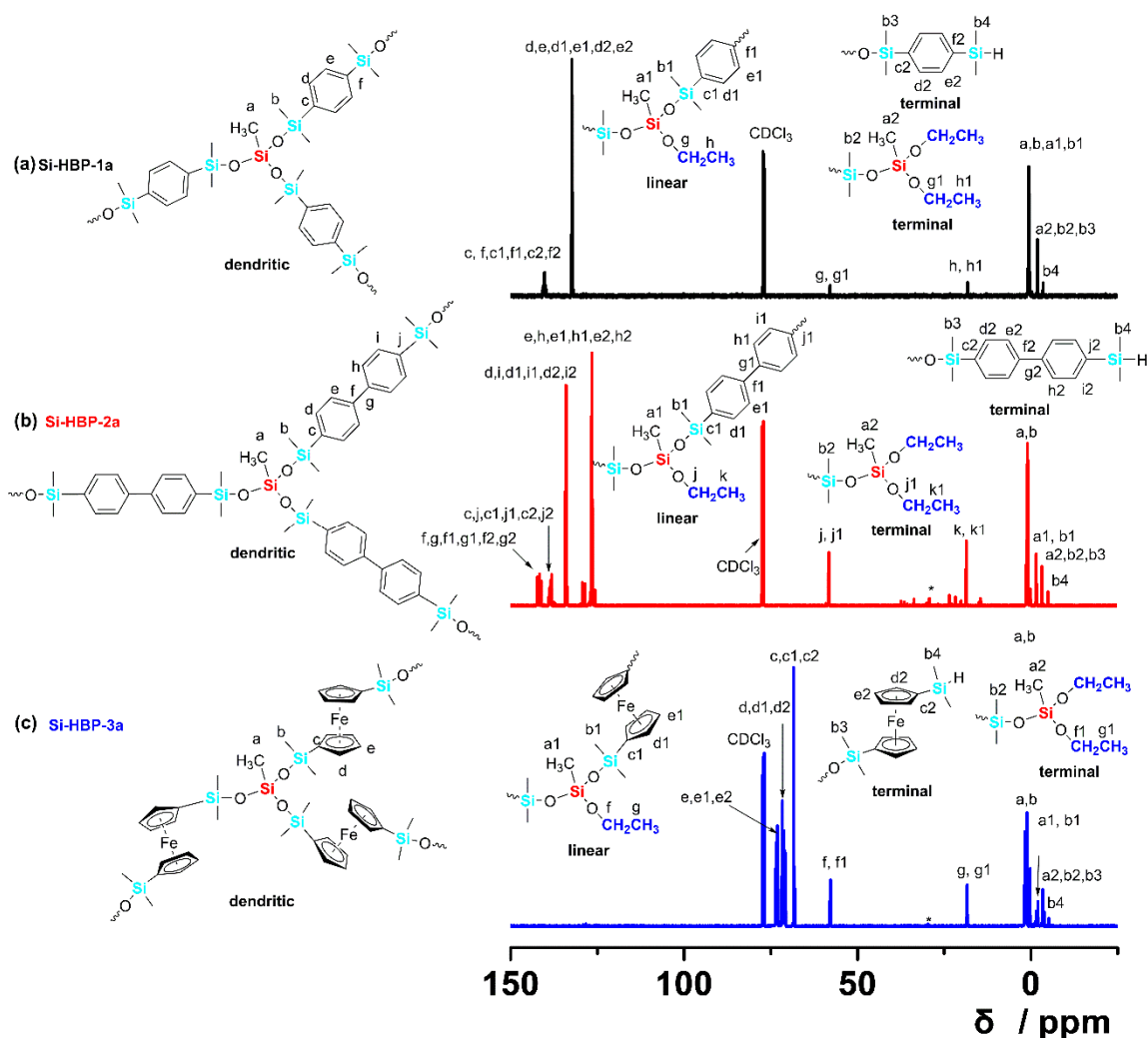


Figure 3. ^{13}C NMR spectra of Si-HBP-1a (a), Si-HBP-2a (b) and Si-HBP-3a (c). The asterisk denotes the residual toluene in the product.

For silicon-containing hyperbranched polymers, ^{29}Si NMR is an important technique to identify the Si chemical environments in the structures. Figure 4a shows the possible Si chemical structures and Figure 4b,c and Figures S5–S7 (Supplementary Materials) show the ^{29}Si NMR spectra of these polymers. For Si-HBP-1a, the silicon atoms linked to three oxygen atoms in the dendritic (Si_a), linear (Si_c) and terminal (Si_g) units are found at ca. -64 , -57 , -49 ppm (Figure 4c). The signals in the region of -0.9 to -2.3 ppm are assigned to silicon atoms linked to two methyl groups (Si_b , Si_d , Si_e , and Si_h) (Figure 4b). However, The Si–H was not detected because of its low amount and weak signals. The results of ^{29}Si NMR spectra for Si-HBP-2a are similar to those for Si-HBP-1a (Figure 4b,c). For Si-HBP-3a, the introduction of ferrocene leads the signals of Si atoms in Si-CH₃ groups to move to the low field in the region of 0.01–0.48 ppm (Figure 4b,c). Similar results are also found in other polymers. In addition, there is a small difference between the calculated and theoretical contents of C and H contents in the elemental analysis. This finding may be due to the presence of terminal units, because the theoretical contents were calculated based on the hypothetically complete reaction between Si–H groups and ethoxy groups.

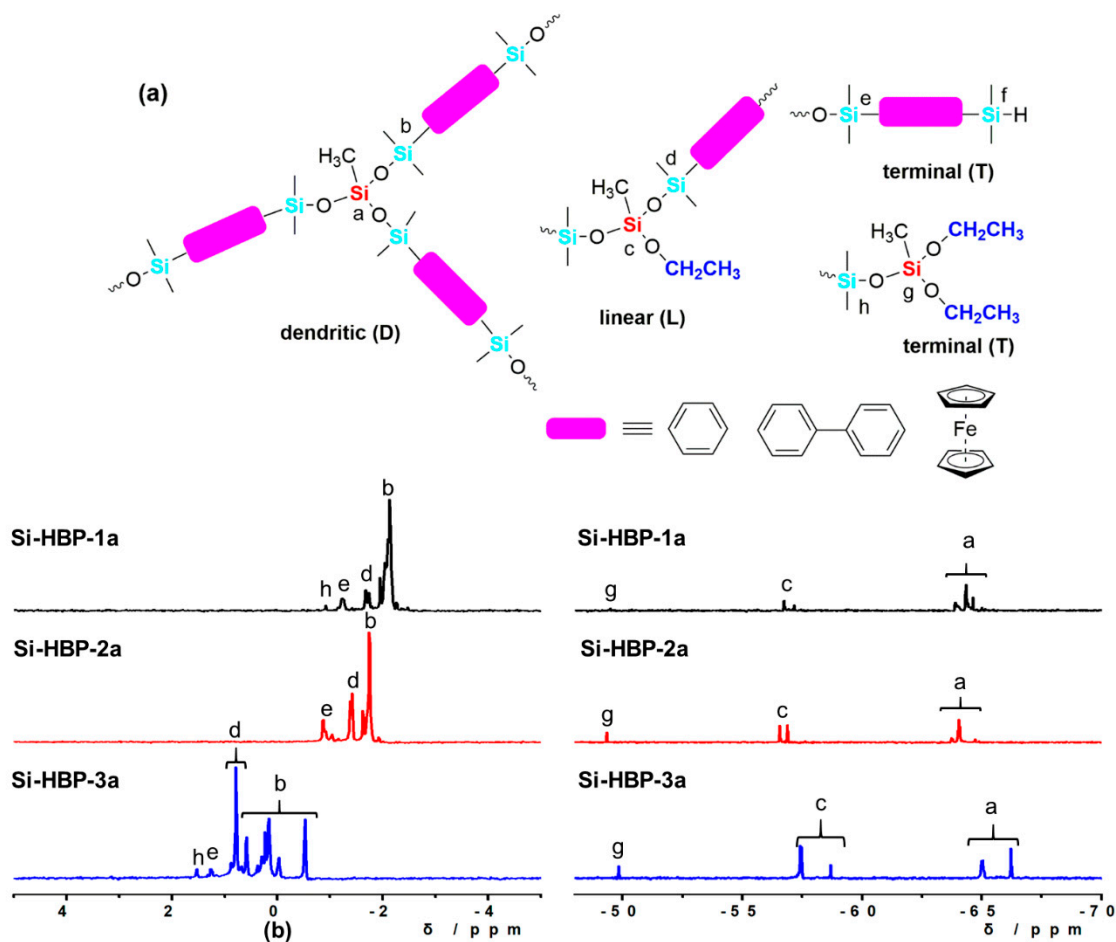


Figure 4. (a) The possible Si chemical environments for Si-HBPs; (b–c) ^{29}Si NMR spectra of Si-HBP-1a, Si-HBP-2a and Si-HBP-3a in the region of 5–−5 ppm (b) and in the region of −48–−70 ppm (c).

Moreover, based on the quantitative ^{29}Si NMR spectroscopy, the degrees of branching (DBs) of these polymers can be determined and calculated according to Equations (1) and (2), based on Frey's and Fréchet's definition [39,40]:

$$\text{DB} = \frac{2D}{2D + L} \quad (1)$$

$$\text{DB} = \frac{D + T}{D + T + L} \quad (2)$$

where D , L , T represent the fraction of dendritic, linear, terminal units in hyperbranched polymers. After calculation, the DBs of these polymers were in the range of 0.69 (Si-HBP-3) to 0.89 (Si-HBP-1) and 0.55 (Si-HBP-3a) to 0.88 (Si-HBP-1b) for DB_{Frey} and $\text{DB}_{\text{Fréchet}}$ (Table 2). The values are similar to other silicon-containing hyperbranched polymers, such as hyperbranched ferrocene-containing poly(boro)carbosilanes (DB_{Frey} : 0.50–0.77; $\text{DB}_{\text{Fréchet}}$: 0.47–0.79) [17], thioether-containing Si-HBP (DB: 0.6) [21]. These results demonstrate that these polymers have highly branched architectures.

The relative molecular weights of these polymers were determined by GPC analysis with polystyrene standards for calibration (Figures S8–S13 in Supplementary Materials). The results are summarized in Table 2. The average molecular weights of these polymers were in the range of 1850 g mol^{-1} (Si-HBP-3b) to 4300 g mol^{-1} (Si-HBP-1a). These values are moderate compared to other silicon-containing hyperbranched polymers [21]. The polydispersity indexes (PDIs) of the resultant polymers were broad and from 2.16 (Si-HBP-3b) to 4.21 (Si-HBP-1a). This phenomenon could be assigned to the features of GPC analysis, which do not always lead to very accurate molecular weight values for hyperbranched polymers. It is interesting that the phenyltriethoxysilane derived

products (Si-HBP-1b, 2b and 3b) possess lower molecular weight than methyltriethoxysilane derived products (Si-HBP-1a, 2a and 3a). This finding can be attributed to the relatively lower reaction activity, due to the higher steric hindrance of phenyltriethoxysilane than that of methyltriethoxysilane. The different molecular weight among them may be due to the different cyclization product in the final network, because the intramolecular cyclization reaction is generally unavoidable in the synthesis of hyperbranched polymers.

Table 2. GPC data of Si-HBP-1 to Si-HBP-3.

Samples	M_n (g mol ⁻¹) ^a	M_w (g mol ⁻¹) ^a	PDI ^a	DB ^b	DB ^c
Si-HBP-1a	4300	18100	4.21	0.89	0.81
Si-HBP-1b	3600	14300	3.97	0.89	0.88
Si-HBP-2a	3000	11800	3.93	0.77	0.65
Si-HBP-2b	2800	10100	3.61	0.84	0.83
Si-HBP-3a	1950	4700	2.41	0.69	0.55
Si-HBP-3b	1850	4000	2.16	0.69	0.61

^a The molecular weights and the polydispersity index (PDI) were determined by gel permeation chromatography (GPC) analysis, with polystyrene standards for calibration. ^b DB_{Frey} was determined by ²⁹Si NMR; ^c DB_{Fréchet} was determined by ²⁹Si NMR.

In addition, the thermal stabilities of the polymers were evaluated by thermogravimetric analysis (TGA) under N₂ at 10 °C/min. All the polymers exhibit high thermal stability with a high decomposition temperature with T_d (5% mass loss) of approximately 350°C (except Si-HBP-1a) and the char yields of >35% at 1000 °C (Figure S14 in Supplementary Materials). The DSC measurements reveal that there is no obvious glass transition temperature (T_g) for any polymer.

3.3. Magnetoceramic from Ferrocene-Based Hyperbranched Polymer Si-HBP-3a

Si-containing hyperbranched polymers are generally good precursors for constructing nanostructured Si-containing ceramic materials. In particular, the introduction of ferrocene in the ceramics could impart them magnetism [41–43]. Thus, Si-HBP-3a was pyrolyzed in a tube furnace at 900°C for 2 h under a steam of nitrogen and the ceramic product was afforded as a black powder with the yield of 45.6%, consistent with the TGA result. It is interesting that the ceramic can be easily attracted by a magnet, which motivated us to explore its structure and the magnetic property.

To gain the chemical composition of the formed ceramic, powder X-ray diffraction (XRD) was carried out (Figure 5a). As expected, the ceramic displays many Bragg reflection peaks, revealing that it possesses different crystalline species. Based on the databases of JCPDS-International Centre for Diffraction Data (ICDD), the serial peaks at 2θ angles, including 20.8°, 26.6°, 30.1°, 33.1°, 35.6°, and 62.6°, etc., are associated with the reflections of SiO₂, SiC, C, Fe₃O₄, and Fe₂O₃ (ICDD data file 46-1045, 29-1129, 26-1076, 89-0691 and 33-0664). These results reveal that the hyperbranched polymer has been successfully pyrolyzed and transformed into a ceramic.

The magnetic property of the resultant ceramic was investigated by using a vibrating sample magnetometer (VSM). The magnetization curve of the ceramic was shown in Figure 5b. As the strength of the externally applied magnetic field increases, the magnetization of the ceramic sharply increases and reaches the saturated magnetization of 14.6 emu g⁻¹. This value was comparable to some Fe-containing ceramics, such as Fe₃Si nanocrystal enriched ceramic (C1) [43] and ceramics from hyperbranched poly(ferrocenylene)s, containing group 14 and 15 elements [44]. In addition, the magnetization plot contains hysteresis, as can be seen in the inset of Figure 5b. The coercivity is found to be 0.12 kOe. These results reveal that the ferrocene-linked hyperbranched polycarbosiloxane is a promising precursor for magnetic ceramics.

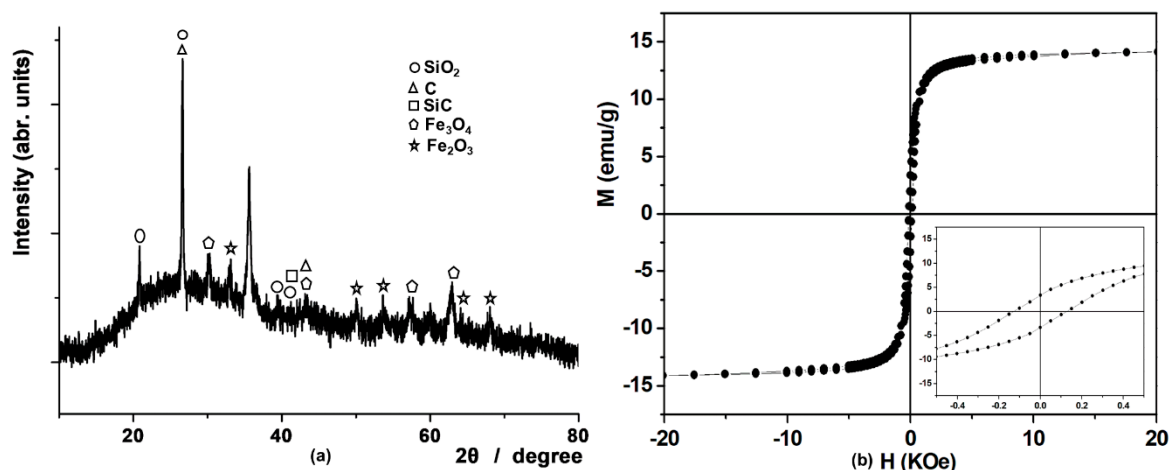


Figure 5. (a) XRD pattern of the ceramic pyrolyzed from Si-HBP-3a; (b) Plot of magnetization (M) versus applied magnetic field (H) at 300 K for the magnetoceramic.

4. Conclusions

In summary, we have prepared a series of novel hyperbranched polycarbosiloxanes by the Piers–Rubinsztajn (P–R) reactions. The polymerization reactions of methyl-, or phenyl- triethoxysilane and three Si-H containing aromatic monomers were carried out at room temperature for 0.5 h, using $B(C_6F_5)_3$ as the catalyst. The structures were proved by FT-IR, 1H NMR, ^{13}C NMR, and ^{29}Si NMR. The molecular weights are in the range of 1850 to 4300 $g\ mol^{-1}$, which are moderate compared to other silicon-containing hyperbranched polymers. The degrees of branching of these polymers were in the range of 0.69–0.89, which were determined by the quantitative ^{29}Si NMR. These polymers can be utilized as precursors for the construction of ceramics. Pyrolysis of a ferrocene-linked Si-HBP at elevated temperature resulted in a ceramic with the yield of 45.6%. The resultant ceramic exhibited a good magnetizability, with the saturation magnetization of 14.6 $emu\ g^{-1}$, which are comparable to those from linear and hyperbranched ferrocene-containing polymers. This work represents a typical example of Si-HBPs prepared by the P–R reactions. The pyrolysis transformation from ferrocene-linked Si-HBP into magnetoceramics imparts them as promising candidates for high-technology applications. More examples could be developed according to this work.

Supplementary Materials: The following are available online at <http://www.mdpi.com/2073-4360/12/3/672/s1>, Figure S1: FT-IR spectroscopy of Si-HBP-1b, Si-HBP-2b and Si-HBP-3b, Figure S2: FT-IR spectroscopy of M-1 and Si-HBP-1a, Figure S3: 1H NMR spectra of Si-HBP-1b (a), Si-HBP-2b (b) and Si-HBP-3b (c), Figure S4: ^{13}C NMR spectra of Si-HBP-1b (a), Si-HBP-2b (b) and Si-HBP-3b (c), Figure S5: ^{29}Si NMR spectra of Si-HBP-1a, Si-HBP-2a and Si-HBP-3a, Figure S6: ^{29}Si NMR spectra of Si-HBP-1b, Si-HBP-2b and Si-HBP-3b, Figure S7: (a) The possible Si chemical environments for Si-HBPs; (b-c) ^{29}Si NMR spectra of Si-HBP-1b, Si-HBP-2b and Si-HBP-3b in the region of 5–5 ppm and in the region of -60–85 ppm, Figure S8: GPC curve of Si-HBP-1a, Figure S9: GPC curve of Si-HBP-1b, Figure S10: GPC curve of Si-HBP-2a, Figure S11: GPC curve of Si-HBP-2b, Figure S12: GPC curve of Si-HBP-3a, Figure S13: GPC curve of Si-HBP-3b. Figure S14: TGA curves of hyperbranched polycarbosiloxanes, Si-HBP-1~Si-HBP-3 under the atmosphere of nitrogen from temperature to 1000 °C.

Author Contributions: Methodology, H.Z., L.X. and Q.M.; formal analysis, H.Z., L.X., J.L., and Q.M.; investigation, H.Z., L.X., J.L. and Q.M.; writing—original draft preparation, Q.M.; writing—review and editing, H.Z., L.X., J.L. and Q.M. All authors have read and agreed to the published version of the manuscript.

Funding: This research was funded by the National Natural Science Foundation of China: 21604077; Natural Science Foundation of Shandong Province: ZR2016EMM07.

Conflicts of Interest: The authors declare no conflict of interest.

References

1. Zhou, Y.; Huang, W.; Liu, J.; Zhu, X.; Yan, D. Self-Assembly of Hyperbranched Polymers and Its Biomedical Applications. *Adv. Mater.* **2010**, *22*, 4567–4590. [[CrossRef](#)]
2. Jiang, W.; Zhou, Y.; Yan, D. Hyperbranched polymer vesicles: From self-assembly, characterization, mechanisms, and properties to applications. *Chem. Soc. Rev.* **2015**, *44*, 3874–3889. [[CrossRef](#)] [[PubMed](#)]
3. Wang, D.; Zhao, T.; Zhu, X.; Yan, D.; Wang, W. Bioapplications of hyperbranched polymers. *Chem. Soc. Rev.* **2015**, *44*, 4023–4071. [[PubMed](#)]
4. Wu, W.; Tang, R.; Li, Q.; Li, Z. Functional hyperbranched polymers with advanced optical, electrical and magnetic properties. *Chem. Soc. Rev.* **2015**, *44*, 3997–4022. [[CrossRef](#)] [[PubMed](#)]
5. Zheng, Y.; Li, S.; Weng, Z.; Gao, C. Hyperbranched polymers: Advances from synthesis to applications. *Chem. Soc. Rev.* **2015**, *44*, 4091–4130. [[PubMed](#)]
6. Zeng, H.; Wang, L.; Zhang, D.; Yan, P.; Nie, J.; Sharma, V.K.; Wang, C. Highly efficient and selective removal of mercury ions using hyperbranched polyethylenimine functionalized carboxymethyl chitosan composite adsorbent. *Chem. Eng. J.* **2019**, *358*, 253–263. [[CrossRef](#)]
7. Chen, H.; Kong, J. Hyperbranched polymers from $A_2 + B_3$ strategy: Recent advances in description and control of fine topology. *Polym. Chem.* **2016**, *7*, 3643–3663. [[CrossRef](#)]
8. Yao, J.Z.; Son, D.Y. Synthesis of an organosilicon hyperbranched oligomer containing alkenyl and silyl hydride groups. *J. Polym. Sci.-Polym. Chem.* **1999**, *37*, 3778–3784. [[CrossRef](#)]
9. Yoon, K.; Son, D.Y. Syntheses of hyperbranched poly(carbosilylenes). *Macromolecules* **1999**, *32*, 5210–5216. [[CrossRef](#)]
10. Rim, C.; Son, D.Y. Hyperbranched poly(carbosilanes) from silyl-substituted furans and thiophenes. *Macromolecules* **2003**, *36*, 5580–5584. [[CrossRef](#)]
11. Arkas, M.; Tsiourvas, D.; Paleos, C.M. Organosilicon dendritic networks in porous ceramics for water purification. *Chem. Mater.* **2005**, *17*, 3439–3444. [[CrossRef](#)]
12. Li, D.; Niu, Y.; Yang, Y.; Wang, X.; Yang, F.; Shen, H.; Wu, D. Synthesis and self-assembly behavior of POSS-embedded hyperbranched polymers. *Chem. Commun.* **2015**, *51*, 8296–8299. [[CrossRef](#)] [[PubMed](#)]
13. Chen, G.W.; Li, W.J.; Zhang, C.; Zhou, C.J.; Feng, S.Y. Preparation of a novel hyperbranched carbosilane-silica hybrid coating for trace amount detection by solid phase microextraction/gas chromatography. *J. Chromatog. A* **2012**, *1256*, 213–221. [[CrossRef](#)] [[PubMed](#)]
14. Feng, Y.; Bai, T.; Yan, H.; Ding, F.; Bai, L.; Feng, W. High Fluorescence Quantum Yield Based on the Through-Space Conjugation of Hyperbranched Polysiloxane. *Macromolecules* **2019**, *52*, 3075–3082. [[CrossRef](#)]
15. Bai, L.; Yan, H.; Bai, T.; Feng, Y.; Zhao, Y.; Ji, Y.; Feng, W.; Lu, T.; Nie, Y. High Fluorescent Hyperbranched Polysiloxane Containing beta-Cyclodextrin for Cell Imaging and Drug Delivery. *Biomacromolecules* **2019**, *20*, 4230–4240. [[CrossRef](#)]
16. Zhao, Z.; Guo, Y.; Jiang, T.; Chang, Z.; Lam, J.W.Y.; Xu, L.; Qiu, H.; Tang, B.Z. A Fully Substituted 3-Silolene Functions as Promising Building Block for Hyperbranched Poly(Silylenevinylene). *Macromol. Rapid Commun.* **2012**, *33*, 1074–1079. [[CrossRef](#)]
17. Kong, J.; Schmalz, T.; Motz, G.; Müller, A.H.E. Novel Hyperbranched Ferrocene-Containing Poly(boro)carbosilanes Synthesized via a Convenient “ $A_2 + B_3$ ” Approach. *Macromolecules* **2011**, *44*, 1280–1291. [[CrossRef](#)]
18. Liu, X.; Rathore, J.S.; Dubois, G.; Interrante, L.V. Grignard Condensation Routes to 1,3-Disilacyclobutane-Containing Cycloliner Polycarbosilanes. *J. Polym. Sci. Polym. Chem.* **2017**, *55*, 1547–1557. [[CrossRef](#)]
19. Migulin, D.; Milenin, S.; Cherkaev, G.; Svidchenko, E.; Surin, N.; Muzafarov, A. Sodiumoxy(aminopropyl) alkoxy silanes- AB_2 type monomers for the synthesis of hyperbranched poly(aminopropyl) alkoxy siloxanes and their derivatives. *J. Organomet. Chemistry* **2018**, *859*, 24–32. [[CrossRef](#)]
20. Zhang, Y.; Zuo, Y.J.; Yang, T.X.; Gou, Z.M.; Lin, W.Y. Polysiloxane-based hyperbranched fluorescent materials prepared by thiolene “click” chemistry as potential cellular imaging polymers. *Eur. Polym. J.* **2019**, *112*, 515–523. [[CrossRef](#)]
21. Xue, L.; Yang, Z.; Wang, D.; Wang, Y.; Zhang, J.; Feng, S. Synthesis and characterization of silicon-containing hyperbranched polymers via thiol-ene click reaction. *J. Organomet. Chem.* **2013**, *732*, 1–7. [[CrossRef](#)]
22. Parks, D.J.; Piers, W.E. Tris(pentafluorophenyl)boron-Catalyzed Hydrosilation of Aromatic Aldehydes, Ketones, and Esters. *J. Am. Chem. Soc.* **1996**, *118*, 9440–9441. [[CrossRef](#)]
23. Rubinsztajn, S.; Cella, J.A. A New Polycondensation Process for the Preparation of Polysiloxane Copolymers. *Macromolecules* **2005**, *38*, 1061–1063. [[CrossRef](#)]

24. Brook, M.A. New Control Over Silicone Synthesis using SiH Chemistry: The Piers–Rubinsztajn Reaction. *Chem. Eur. J.* **2018**, *24*, 8458–8469. [[CrossRef](#)] [[PubMed](#)]
25. Chen, X.; Yi, M.; Wu, S.; Tan, L.; Ge, X.; He, M.; Yin, G. Synthesis of Structurally Precise Polysiloxanes via the Piers–Rubinsztajn Reaction. *Materials* **2019**, *12*, 304. [[CrossRef](#)] [[PubMed](#)]
26. Sample, C.S.; Lee, S.-H.; Bates, M.W.; Ren, J.M.; Lawrence, J.; Lensch, V.; Gerbec, J.A.; Bates, C.M.; Li, S.; Hawker, C.J. Metal-Free Synthesis of Poly(silyl ether)s under Ambient Conditions. *Macromolecules* **2019**, *52*, 1993–1999. [[CrossRef](#)]
27. Schneider, A.F.; Brook, M.A. High-Throughput Synthesis and Characterization of Aryl Silicones by Using the Piers–Rubinsztajn Reaction. *Chem. Eur. J.* **2019**, *25*, 15367–15374. [[CrossRef](#)]
28. Ai, L.; Chen, Y.; He, L.; Luo, Y.; Li, S.; Xu, C. Synthesis of structured polysiloxazanes via a Piers–Rubinsztajn reaction. *Chem. Commun.* **2019**, *55*, 14019–14022. [[CrossRef](#)]
29. Yi, M.; Chen, X.; Wu, S.; Ge, J.; Zhou, X.; Yin, G. Fabrication of Reactive Poly(Phenyl-Substituted Siloxanes/Silsesquioxanes) with Si–H and Alkoxy Functional Groups via the Piers–Rubinsztajn Reaction. *Polymers* **2018**, *10*, 1006. [[CrossRef](#)]
30. Macphail, B.; Brook, M.A. Controlling silicone–saccharide interfaces: Greening silicones. *Green Chem.* **2017**, *19*, 4373–4379. [[CrossRef](#)]
31. Zhang, J.; Chen, Y.; Sewell, P.; Brook, M.A. Utilization of softwood lignin as both crosslinker and reinforcing agent in silicone elastomers. *Green Chem.* **2015**, *17*, 1811–1819. [[CrossRef](#)]
32. Yu, J.Y.; Liu, Y.Z. Cyclic Polysiloxanes with Linked Cyclotetrasiloxane Subunits. *Ang. Chem. Int. Ed.* **2017**, *56*, 8706–8710. [[CrossRef](#)] [[PubMed](#)]
33. Matsumoto, K.; Oba, Y.; Nakajima, Y.; Shimada, S.; Sato, K. One-Pot Sequence-Controlled Synthesis of Oligosiloxanes. *Ang. Chem. Int. Ed.* **2018**, *57*, 4637–4641. [[CrossRef](#)] [[PubMed](#)]
34. Liu, N.; Yu, J.Y.; Meng, Y.Y.; Liu, Y.Z. Hyperbranched Polysiloxanes Based on Polyhedral Oligomeric Silsesquioxane Cages with Ultra-High Molecular Weight and Structural Tuneability. *Polymers* **2018**, *10*, 496. [[CrossRef](#)]
35. Wu, C.Y.; Hu, C.H.; Liu, Y.Z. Hyperbranched polysiloxane with highly constrained rings and the effect of the attached arms on the assembly behavior. *Polym. Chem.* **2017**, *8*, 6490–6495. [[CrossRef](#)]
36. Chojnowski, J.; Rubinsztajn, S.; Fortuniak, W.; Kurjata, J. Synthesis of Highly Branched Alkoxysiloxane–Dimethylsiloxane Copolymers by Nonhydrolytic Dehydrocarbon Polycondensation Catalyzed by Tris(pentafluorophenyl)borane. *Macromolecules* **2008**, *41*, 7352–7358. [[CrossRef](#)]
37. Grande, J.B.; Urlich, T.; Dickie, T.; Brook, M.A. Silicone dendrons and dendrimers from orthogonal SiH coupling reactions. *Polym. Chem.* **2014**, *5*, 6728–6739. [[CrossRef](#)]
38. Chen, H.; Kong, J.; Tian, W.; Fan, X.-D. Intramolecular Cyclization in A₂ + B₃ Polymers via Step-Wise Polymerization Resulting in a Highly Branched Topology: Quantitative Determination of Cycles by Combined NMR and SEC Analytics. *Macromolecules* **2012**, *45*, 6185–6195. [[CrossRef](#)]
39. Frey, H.; Hölter, D. Degree of branching in hyperbranched polymers. 3 Copolymerization of AB_m-monomers with AB and AB_n-monomers. *Acta Polym.* **1999**, *50*, 67–76. [[CrossRef](#)]
40. Hawker, C.J.; Lee, R.; Frechet, J.M.J. One-step synthesis of hyperbranched dendritic polyesters. *J. Am. Chem. Soc.* **1991**, *113*, 4583–4588. [[CrossRef](#)]
41. Li, H.; Chi, W.; Liu, Y.; Yuan, W.; Li, Y.; Li, Y.; Tang, B.Z. Ferrocene-Based Hyperbranched Polytriazoles: Synthesis by Click Polymerization and Application as Precursors to Nanostructured Magnetoceramics. *Macromol. Rapid Commun.* **2017**, *38*, 1700075. [[CrossRef](#)] [[PubMed](#)]
42. Kong, J.; Kong, M.; Zhang, X.; Chen, L.; An, L. Magnetoceramics from the Bulk Pyrolysis of Polysilazane Cross-Linked by Polyferrocenylcarbosilanes with Hyperbranched Topology. *ACS Appl. Mater. Interface* **2013**, *5*, 10367–10375. [[CrossRef](#)] [[PubMed](#)]

43. Kong, J.; Schmalz, T.; Motz, G.; Muller, A.H.E. Magnetoceramic nanocrystals from the bulk pyrolysis of novel hyperbranched polyferrocenyl(boro)carbosilanes. *J. Mater. Chem. C* **2013**, *1*, 1507–1514. [[CrossRef](#)]
44. Häußler, M.; Sun, Q.; Xu, K.; Lam, J.W.Y.; Dong, H.; Tang, B.Z. Hyperbranched Poly(ferrocenylene)s Containing Groups 14 and 15 Elements: Syntheses, Optical and Thermal Properties, and Pyrolytic Transformations into Nanostructured Magnetoceramics. *J. Inorg. Organomet. Polym. Mater.* **2005**, *15*, 67–81. [[CrossRef](#)]



© 2020 by the authors. Licensee MDPI, Basel, Switzerland. This article is an open access article distributed under the terms and conditions of the Creative Commons Attribution (CC BY) license (<http://creativecommons.org/licenses/by/4.0/>).